Performance Analysis Of Multi Source Fused Medical Images Using Multiresolution Transforms

Ch.Hima Bindu[1]
[1] Assoc. Professor, ECE Department, QIS College of Engineering & Technology, Ongole, Andhra Pradesh,

Dr K.Satya Prasad[2]
[2]Rector& Professor of ECE Department, JNTUK, Kakinada, Andhra Pradesh, India.

***Abstract*— Image fusion combines information from multiple images of the same scene to get a composite image that is more suitable for human visual perception or further image-processing tasks. In this paper the multi source medical images like MRI (Magnetic Resonance Imaging), CT (computed tomography) & PET (positron emission tomography) are fused using different multi scale transforms. We compare various multi resolution transform algorithms, especially the latest developed methods, such as; Non Subsampled Contourlet Transform, Fast Discrete Curvelet, Contourlet, Discrete Wavelet transform and Hybrid Method (combination of DWT & Contourlet) for image fusion. The fusion operations are performed with all Multi resolution transforms. The fusion rules like local maxima and spatial frequency techniques are used for selection in the low frequency and high frequency subband coefficients, which can preserve more information and quality in the fused image. The fused output obtained after the inverse transform of fused sub band coefficients. The experimental results show that the effectiveness of fusion approaches in fusing multi source images.**

Keywords- Image Fusion; Discrete Wavelet Transform; Contourlet Transform; Fast Discrete Curvelet Transform; Nonsubsampled Contourlet Transform.

I. INTRODUCTION

The Image fusion is the process of combining information from two or more images of a scene into a single composite image which is more informative and is more suitable for visual perception or computer processing. The objective in the image fusion is to reduce uncertainty and minimize redundancy in the output, while maximizing relevant information particular to an application or task as well. Given the same set of input images, different fused images may be created depending on the specific application and what is considered as relevant information. There are several benefits in using image fusion: wider spatial and temporal coverage with decreased uncertainty, improved reliability and increased robustness of system performance [Ref.3].

The medical images like MRI and CT provides high-resolution images with structural and anatomical information. PET images provide functional information with low spatial resolution. In the recent years, the success of MRI-CT, PET-MRI [Ref.1] & PET-CT [Ref.6] imaging in the clinical field triggered considerable interest in noninvasive functional and anatomical imaging. The limited spatial resolution in PET images is often resulted unsatisfactory in morphological analysis. Combining anatomical and functional tomography datasets provide much more qualitative detection and quantitative determination in this area [Ref .1, Ref .10].

So far, several fusion algorithms based on multi source medical images have been proposed. The MRI-CT image fusion using edge preserved technique proposed by Xianghi et al, based on multi scale toggle contrast operator [Ref .4]. The MRI-PET image fusion proposed by Sabalan Daneshvar et al based on combining HIS (Hue Intensity Saturation model) and retina models improve the functional and spatial information content [Ref .1]. The CT-PET image fusion proposed by Yuhui Liu et al, based on multi wavelet transform adds more details and structure information [Ref .6].

The rest of the paper is organized as follows: Section 2 explains Multiscale transforms. Section 3 presents generic fusion model. Section 4 explains the proposed method. Section 5 the discussion on the experimental results. In the laconic section, the paper is concluded.

II. MULTIRESOLUTION TRANSFORMATIONS

A. Discrete Wavelet Transform

Discrete Wavelet transform (DWT) provides a framework in which a signal is decomposed, with each level corresponding to lower frequency sub band, and higher frequency sub bands. There are two main groups of transforms: continuous and discrete. In one dimension the idea of the wavelet transform is to present the signal as a superposition of wavelets. If a signal is represented by f (t), the wavelet decomposition is

$$f(t) = \sum_{m,n} c_{m,n} \psi_{m,n}(t) \tag{2.1}$$

Where $\psi_{m,n}(t) = 2^{-m/2} \psi\left(2^{-m} t - n\right)$, m and n are integers. There exist very special choices of ψ such that $\psi_{m,n}(t)$ constitutes an ortho normal basis, so that the wavelet transform coefficient can be obtained by an inner calculation:

$$c_{m,n} = \langle f, \psi_{m,n} \rangle = \int \psi_{m,n}(t) f(t) dt \tag{2.2}$$

In order to develop a multiresolution analysis, a scaling function ϕ is needed, together with the dilated and translated parameters of $\phi_{m,n}(t) = 2^{-m/2} \phi\left(2^{-m} t - n\right)$. The signal $f(t)$ can be decomposed in its coarse part and details of various sizes by projecting it onto the corresponding spaces. Therefore, the approximation coefficients $a_{m,n}$ of the

function f at resolution 2^m and wavelet coefficients $c_{m,n}$ can be obtained:

$$a_{m,n} = \sum_k h_{2n-k} a_{m-1,k} \quad (2.3)$$

$$C_{m,n} = \sum_k g_{2n-k} a_{m-1,k} \quad (2.4)$$

Where h_n is a low pass FIR filter and g_n is a high pass FIR filter. To reconstruct the original signal, the analysis filter can be selected from a biorthogonal set which have a related set of synthesis filters. These synthesis filters $\tilde{h}$ and $\tilde{g}$ can be used to perfectly reconstruct the signal using the reconstruction formula

$$a_{m-1,l}(f) = \sum_n \left[\tilde{h}_{2n-l} a_{m,n}(f) + \tilde{g}_{2n-l} c_{m,n}(f) \right] \quad (2.5)$$

Equations (2.3) and (2.4) are implemented by filtering and down sampling. Conversely equation (2.5) is implemented by an initial up sampling and a subsequent filtering.

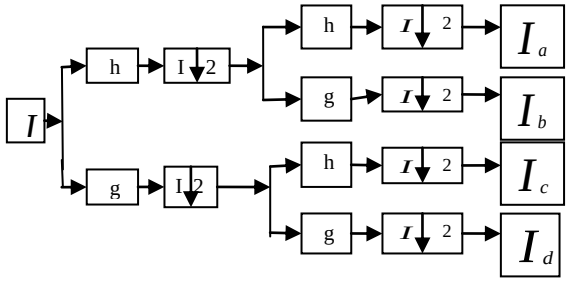

Fig 1: Structure of 2-D DWT

In a 2-D DWT, a 1-D DWT is first performed on the rows and then columns of the data by separately filtering and down sampling. This result in one set of approximation coefficients I_a and three set of detail coefficients, as shown in Fig 1, where I_b, I_c, I_d represent the horizontal, vertical and diagonal directions of the image I, respectively.

In the filter theory, these four sub images correspond to the outputs of low-low (**LL**), low-high (**LH**), high-low (**HL**), and high-high (**HH**) bands. By recursively applying the same scheme to the LL sub band multi resolution decomposition with a desire level can then be achieved. There, a DWT with K decomposition levels will have M=3*K+1 such frequency bands.

B. *Contourlet Transform*

The contourlet transform is first developed in continuous domain and then is discretized for sampled data; contoured transform starts with a discrete domain construction. The contourlet is also deemed as a "true" two dimensional transform that can capture the intrinsic geometrical structure of an image. Two filter banks are employed to implement the contoured transform as shown in Fig.2.

The Laplacian pyramid is first used to capture the point discontinuities, and then a directional filter bank is used to link point discontinuities into linear structures. As the DWT, the contoured transform also has no shift invariant property because of the down-sampling operation.

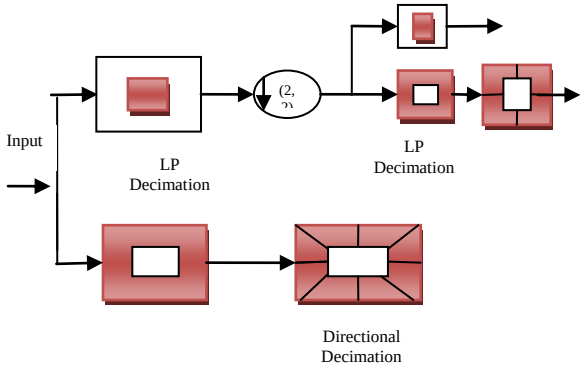

Fig 2: Block diagram of contourlet transform

Do and Vetterli found that to obtain a sparser representation for 2-D piecewise smooth functions in R2, an effective method is to utilize a double filter bank scheme, that is, first apply a multiscale decomposition to capture point discontinuities and then perform a local directional decomposition to synthesize the nearby edge points into independent contour segments.

With a rich set of basis oriented at various directions and scales, contourlet can effectively capture the intrinsic contours and edges in natural images that set radiational multiresolution analysis methods are difficult to handle. Contourlet offer s a much richer sub band set of different directions and shapes, which helps to capture geometric structures in images much more efficiently [Ref.7].

C. *Non Subsampled Contourlet Transform (NSCT)*

In the foremost contourlet transform down samplers and up samplers are presented in both the laplacian pyramid and the Directional Filter Bank (DFB). Thus, it is not shift-invariant, which causes pseudo-Gibbs phenomena around singularities. NSCT is an improved form of contourlet transform. It is motivated to be employed in some applications, in which redundancy is not a major issue, i.e. image fusion. In contrast with contourlet transform, non subsampled pyramid structure and non subsampled directional filter banks are employed in NSCT. The non subsampled pyramid structure is achieved by using two-channel non subsampled 2-D filter banks. The DFB is achieved by switching off the downsamplers/up samplers in each two-channel filter bank in the DFB tree structure and up sampling the filters accordingly. As a result, NSCT is shift-invariant and leads to better frequency selectivity and regularity than contourlet transform. Fig.3 shows the decomposition framework of contourlet transform and NSCT [Ref.11]. The NSCT structure consists in a bank of filters that splits the 2-D frequency plane in the subband; these are a non subsampled pyramid structure that ensures the Multiscale property and a non subsampled directional filter bank structure that gives directionality [Ref.15].

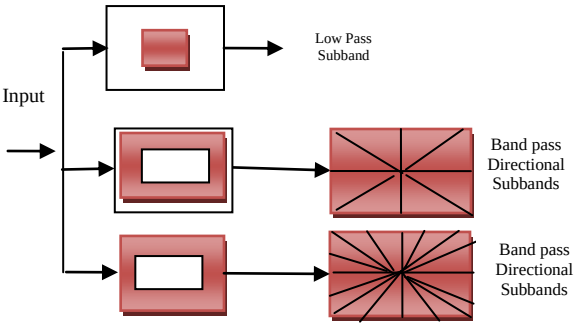

Fig 3: Block diagram of NSCT

A. Curvelet Transform

The DWT, SWT, and DTCWT cannot capture curves and edges of images. More reasonable bases should contain geometrical structure information when they are used to represent images. Candes and Donoho proposed the Curvelet transform (CVT) with the idea of representing a curve as a superposition of bases of various lengths of width obeying the scaling width ≈ length . The CVT is referred to as the ‘‘true” 2D transform. The discrete version implemented in this is a ‘‘wrapping” transform. The second generation of Curvelet transform is presented in Fig: 4. Firstly, the 2D FFT is applied to the source image to obtain Fourier samples. Next, a discrete localizing window smoothly localizes the Fourier transform near the sheared wedges obeying the parabolic scaling. Then, the wrapping transformation is applied to re-index the data. Finally, the inverse 2D FFT is used to obtain the discrete CVT coefficients [Ref.16].

Fig 4: The second generation of Curvelet transforms

III. HYBRID METHOD

The hybrid method can be referred from [Ref.2, Ref.17] references. In this paper reference [Ref.17] method is considered as basic method to do further comparisons.

IV. GENERIC MODEL OF MULTISCALE-BASED IMAGE FUSION

In this paper, there are two different input medical source images A and B (like MRI & CT, MRI & PET, CT & PET). The image fusion algorithm should preserve all the salient features of source images. Fig 5 illustrates the generic image fusion frame work based on Multiscale image decomposition methods. The source images are firstly decomposed into low-frequency sub bands and a sequence of high-frequency sub bands in different scales and orientations. Then the fusion coefficients are obtained from sub bands according to fusion rules. Finally, fused image is reconstructed by applying inverse transform on the fused sub bands.

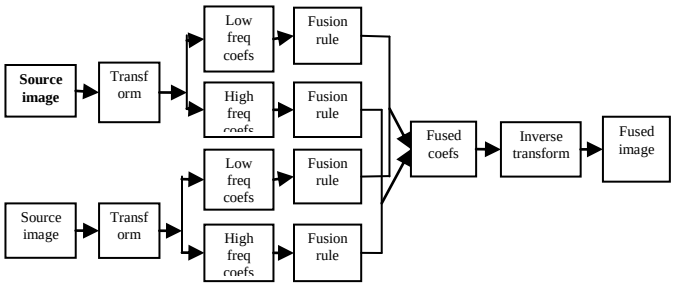

Fig 5: Block diagram of generic model of multi scale image fusion

The key issue in spatial domain algorithms is identifying the most important information in source images and fusing the salient information into the fused image [Ref.8]. This paper includes the average pixel method and PCA method. The fusion rules are explained in the following sections.

A. Fusion rule of lower sub band coefficients

The coefficients in the coarsest scale sub band represent the approximation component of the source image. It is a smooth and sub sampled version of the original image. Therefore, most of the source images information is kept in low frequency bands. The proposed selection principles for the sub band coefficients are finally defined as the maximum selection rule is:

$$I_L^F(i,j)=\begin{cases} I_L^A(i,j) & if: I_L^A(i,j) > I_L^B(i,j) \\ I_L^B(i,j) & if: I_L^A(i,j) \le I_L^B(i,j) \end{cases} \quad (4.1)$$

B. Fusion rule of higher sub band coefficients

The highpass sub band coefficients represent the detailed components of the source image; according to characteristic of HVS. So, it is easy to find that for the high resolution region the human visual interest is concentrated on the detection of changes in between regional contrast. Then spatial frequency measures in the overall activity an image is present. Therefore, we propose a scheme by computing the spatial frequency method in a neighbourhood to select the high frequency coefficients. The spatial frequency (SF), is originated from the HVS, indicates the overall active level in an image and measure the variation of pixels [9]. For an M x N image I, with gray value I (i, j) at position (i, j) the spatial frequency is defined as

$$SF=\sqrt{(RF)^2+(CF)^2} \quad (4.2)$$

Where RF and CF are the row frequency and column frequency respectively:

$$RF=\sqrt{\frac{1}{MN}\sum_{i=1}^{M}\sum_{j=2}^{N}\left[I(i,j)-I(i,j-1)\right]^2} \quad (4.3)$$

$$CF=\sqrt{\frac{1}{MN}\sum_{i=1}^{N}\sum_{j=2}^{M}\left[I(i,j)-I(i-1,j)\right]^2} \quad (4.4)$$

Each image is partitioned into BxB blocks. The said blocks value varies according to the interest of the user, we consider 8x8 as a block size to obtain more accurate values. Then, compare the spatial frequencies of two corresponding coefficient values in each blocks of I^{A}_{HIGH} and I^{B}_{HIGH} to construct the new block of fused image I^{F}_{HIGH} .

$$I^{F}_{HIGH}(m,n)=\begin{cases} I^{A}_{HIGH}(m,n) & if: SF^{A}_{HIGH} > SF^{B}_{HIGH} \\ I^{B}_{HIGH}(m,n) & if: SF^{A}_{HIGH} < SF^{B}_{HIGH} \\ \dfrac{I^{A}_{HIGH}(m,n)+I^{B}_{HIGH}(m,n)}{2} & otherwise \end{cases} \quad (4.5)$$

V. PROPOSED METHOD

The performance comparison of Multiscale transform method has accomplished the following Steps:

- Decompose the source images A and B into low frequency subband and a series of high frequency sub bands at L levels by using various Multiscale transforms.
- Fuse the low frequency subband coefficients and high frequency subband coefficients according to lower subband fusion rule equation (4.1) and higher subband fusion rules equation (4.2-4.5).
- Reconstruct the original image based on the new fused coefficients of sub bands by taking respective inverse Multiscale Transform, thus fused image is obtained.
- Compare the obtained fused image from various transforms with different evaluation parameters from equation (6.1-6.10).

VI. EXPERIMENTAL RESULTS AND ANALYSIS

To evaluate the performance of the multi scale transforms, several experimental results are presented in this section. Experiments are performed on three different multisource images MRI, CT & PET. The MRI and PET images are downloaded from the Harvard university site (http:// www.med.harvard.edu/ AANLIB/ home.html). Similarly the CT and MRI images are downloaded from www.imagefusion.org website link. The proposed method is applied to these image sets. To show the effectiveness of the multi scale transform the comparisons start with simple basic average method, PCA (principal component analysis) method and Brovery method under spatial domain techniques and DWT [Ref.13-14], Contourlet Transform[Ref.5], Hybrid Method is combination of DWT & Contourlet [Ref.2, Ref.12] and Non subsampled contourlet transform in transform domain techniques. The fused image output based on different methods is shown from Fig 6 – 8. The performances of fused medical images are shown in Fig: 9 using Multiscale transform with different evaluation parameters.

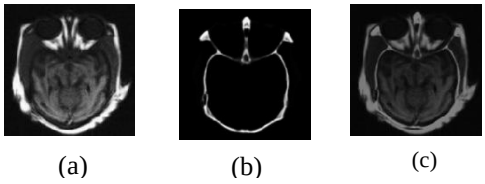

(a) (b) (c)

Fig 6: MRI-CT fusion results (a) Source image A (MRI) (b) Source image (CT) (c) Fused image.

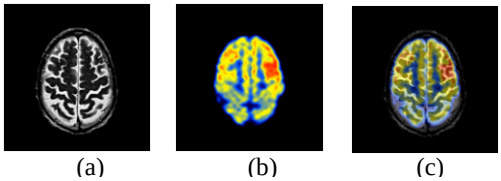

(a) (b) (c)

Fig 7: MRI-PET fusion results (a) Source image A (MRI) (b) Source image B (PET) (c) Fused image.

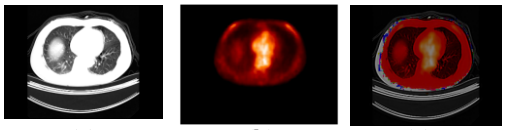

(a) (b) (c)

Fig 8: CT-PET fusion results: (a) Source image A (CT) (b) Source image (PET) (c) Fused image.

A. Peak Signal to Noise Ratio (PSNR)

PSNR (Peak Signal to Noise Ratio) is a metric for the ratio between the maximum possible power of a signal and power of corrupting noise that affects the fidelity of its representation. It is used to measure the quality of reconstructed images.

$$PSNR = 10\log_{10}\left(\frac{L^2}{\frac{i}{M\times N}\sum_{i=1}^{M}\sum_{j=1}^{N}\left(R(i,j)-I^{F}(i,j)\right)^2}\right) \quad (6.1)$$

Where $R(i,j)$ and $I^{F}(i,j)$ are the pixel values of the ideal reference and the obtained fused image, respectively. M and N are the dimensions of the images.

B. Mutual Information (MI)

Mutual information of two random variables is a quantity that measures the mutual dependence of the two variables. Here, $MI_{RI}{}^{F}$ measures the information that reference and the fused image shares:

$$MI_{RIF} = \sum_{i=1}^{L}\sum_{j=1}^{L} P_{RIF}(i,j)\log_2\frac{P_{RIF}(i,j)}{P_R(i)P_{IF}(j)} \quad (6.2)$$

Where P_{RI} is the normalized joint gray level histogram of images R and I^{F}, P_R and P_{I^F} are the normalized marginal histograms of the two images.

The mutual information I_{AF} between the sources images A and the fused image F is defined as follows:

$$I_{AF} = \sum_{AF} P_{AF}(a, f) \log \frac{P_{AF}(a, f)}{P_A(a) P_F(f)} \quad (6.3)$$

Where P_{AF} is the jointly normalized histogram of A and F, P_A and P_F are the normalized histogram of A and F, and a f represent the pixel value of the image A and F, respectively. The mutual information I_{BF} between the source image B and the fused image F are similar to I_{AF} . The mutual information between the source images A, B, and the fused image F is the sum of I_{AF} and I_{BF} , i.e.

$$MI_F^{AB} = I_{AF} + I_{BF} \quad (6.4)$$

C. Gradient and Wrap

The gradient value and wrap values are facilitate the correlation between the resultant F and reference R images. If gradient value is high and wrap value is low then the two images are more correlated. The gradient and warp are defined as follows:

$$Grad = 1/M * N \frac{\sum\sum \sqrt{[F(i,j) - F(i+1,j)]^2 + [F(i,j) - F(i,j+1)]^2}}{\sqrt{2}} \quad (6.5)$$

$$Wrap = 1/M * N \sum_{i=1}^{M} \sum_{j=1}^{N} F(i,j) - R(i,j) \quad (6.6)$$

Where M and N are size of the image.

D. Effective Great Degrees

This is because that the metrics $Q^{AB/F}$ and Q_0 mainly measure the amount of salient information transferred from source images into the fused image [Ref.17]. The metric $Q^{AB/F}$ is defined as follows:

$$Q^{AB/F} = \frac{\sum_{n=1}^{N}\sum_{m=1}^{M}\left(Q^{AF}(n,m)W^A(n,m) + Q^{BF}(n,m)W^B(n,m)\right)}{\sum_{n=1}^{N}\sum_{m=1}^{M}\left(W^A(n,m) + W^B(n,m)\right)} \quad (6.7)$$

The dynamic range of $Q^{AB/F}$ is [0 1], and it should be as close to 1 as possible.

Another metric Q_O is as follows:

$$Q_O(A,F) = \frac{2\sigma_{af}\, 2\bar{a}\,\bar{f}}{(\sigma_a^2 + \sigma_f^2)(\bar{a}^2 + \bar{f}^2)} \quad (6.8)$$

Where σ_{af} represents the coherence between A and F, σ_a σ_f denote the standard deviation of A and F: $\bar{a}$, $\bar{f}$ represent the mean value of A and F respectively, similarly calculate Q_o(B,F) using above equation then finally the Q_0 value is as follows:

$$Q_0 = \frac{Q_0(A,F) + Q_0(B,F)}{2} \quad (6.9)$$

The Q_0 range is $-1 \leq Q_0 \leq 1$ and it should be also as close to 1 as possible.

E. Correlation

It computes the correlation coefficient between fused image F and reference image R. to computes the correlation coefficient using following equation:

$$corr = \frac{\sum_{i}^{M}\sum_{j}^{N}(F(i,j) - \bar{F})(R(i,j) - \bar{R})}{\sqrt{(\sum_{i}^{M}\sum_{j}^{N}\left(F(i,j) - \bar{F}\right)^2)\sum_{i}^{M}\sum_{j}^{N}(\left(R(i,j) - \bar{R}\right)^2)}} \quad (6.10)$$

Where $\bar{F}$ and $\bar{R}$ are mean values of fused and reference images respectively.

For Table I-III refer Appendix A and The graphical representation of all performance evaluation parameters are hown below (Fig 9):

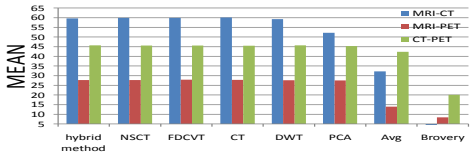

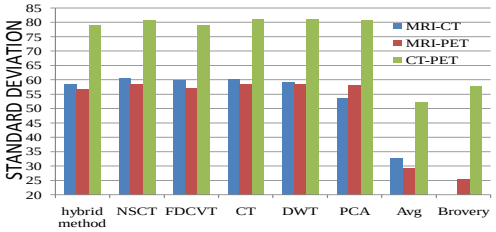

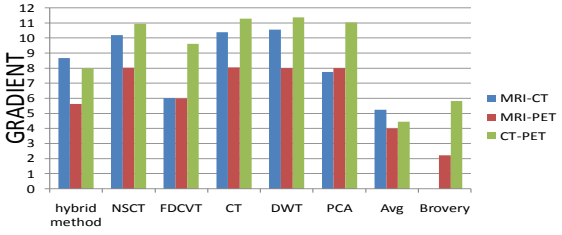

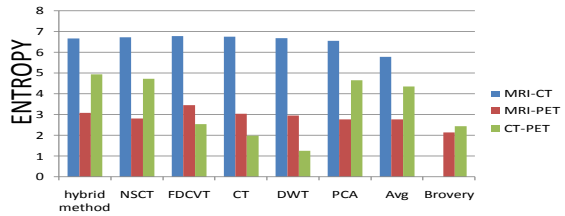

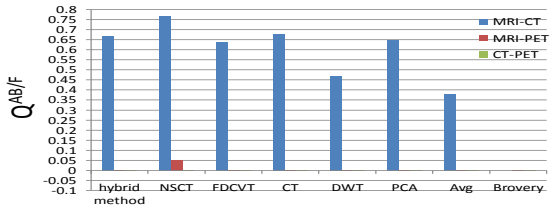

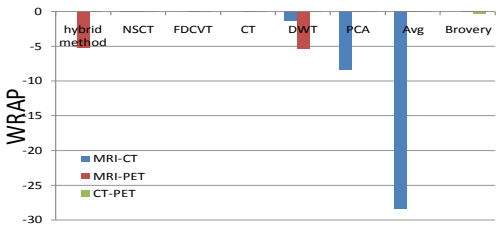

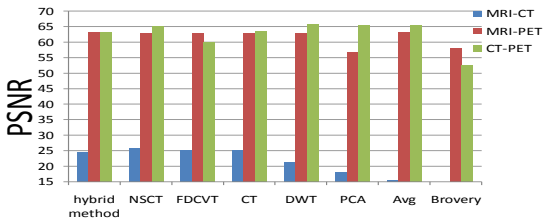

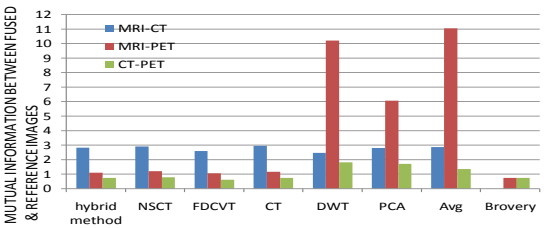

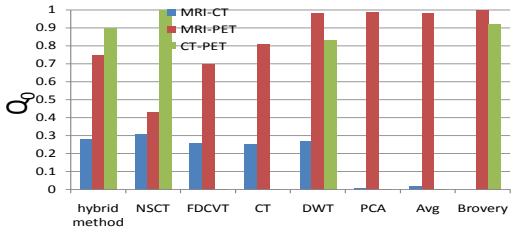

Fig: 9: Performance of fused medical image using different Multiscale transforms with different evaluation parameters.

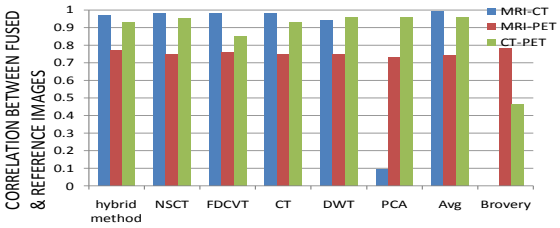

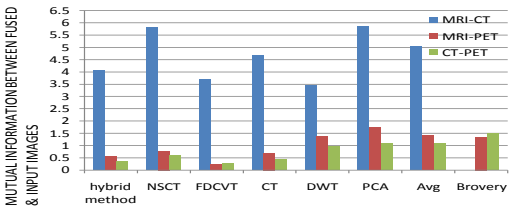

VII. Conclusion

In this paper, performance analysis is compared with different multi scale transforms for the fusion of multi source images. The fusion procedure is discussed with different subband fusion rules to obtain fused image from different multi sources. The obtained fusion results are compared with different evaluation parameters. The comparison of transform methods are starts with those of the pixel averaging, PCA method and Brovery methods. Finally those compared with DWT, Contourlet, Hybrid Method (is combination of DWT & Contourlet), Fast Discrete Curvelet and NSCT fusion methods. We calculated and analyzed tools such as; PSNR, MI, Effective great degrees, gradient, wrap, standard deviation, mean and entropy values.

References

[1] G. Eason, B. Noble, and I. N. Sneddon, “On certain integrals of Lipschitz-Hankel type involving products of Bessel functions,” Phil. Trans. Roy. Soc. London, vol. A247, pp. 529–551, April 1955. (references) Sabalan Daneshvar, Hassan Ghassemian, MRI and PET Image Fusion by Combining HIS and retina – inspired Models, Information Fusion 11, 2010, pp.114-123.

[2] Shutao Li, Bin Yang, Multifocus Image Fusion by Combining Curvelet and Wavelet Transform, Pattern Recognition Letters 29 , 2008, pp.1295-1301.

[3] Guest Editorial, Image Fusion: Advances in the State Of The Art, Information Fusion 8, 2007, pp.114-118.

[4] Xiangzhi Bai, Fugen Zhou, Bindang Xue, Edge Preserved Image Fusion Based on Multiscale Toggle Contrast Operator, Image And Vision Computing 29, 2011, pp. 829-839.

[5] L.Yang, B.L.Guo, W.Ni, Multimodality Medical Image Fusion based on Multiscale Geometric Analysis of Contourlet Transform, Neurocomputing 72, 2008, pp. 203-211.

[6] G.G.Bhutada, R.S.Anand, S.C. Saxena, Edge Preserved Image Enhancement using Adaptive Fusion of Images Denosied By Wavelet And Curvelet Transform, Digital Signal Processing 21 (2011) 118-130.

[7] Yi Chai, Huafeng Li, Xiaoyang Zhang, Multifocus Image Fusion based on features Contrast of Multiscale products in nonsubsampled Contourlet Transform Domain, Optik 123 2012, pp.569-581.

[8] Xiaoquing Zhang, Yongguo Zheng, Yanjun Peng, Weike Liu, Changqiang Yang, Research on multi-mode medical image fusion algorithm based on wavelet transform and edge characteristics of images, 2nd International conference on Image and signal processing, 2009, pp.1-4.

[9] Yuhui Liu, Jinzhu Yang, Jinshan Sun, PET/CT Medical Image Fusion Algorithm Based On Multiwavelet Transform, 2nd International conference on advanced computer and control, 2010, pp.264-268.

[10] I.Pitas, Digital Image processing Scheme and Application, john wiley & sons. New York, 2000.

[11] A.Soma Sekhar, Dr.M.N. Giri Prasad, A Novel Approach Of Image Fusion On MR And CT Images Using Wavelet Transforms, Proc. Of IEEE ICECIT 3rd International Conference, July 2011, pp. 172-176.

[12] M.N.Do, M.Verrerli, The contourlet transform: an efficient directional multi resolution image representation, IEEE Trans. On Image Processing 14(12), 2005, pp.2091-2106.

[13] G.Piella, A General Framework for Multi resolution image Fusion: From Pixels to Regions. Information Fusion (4), 2003, pp.259-280.

[14] S.T.Li,b.Yang, Multifocus Image Fusion Using Region Segmentation and Spatial Frequency, Image and Vision Computing 26 (7) ,2008, pp. 971-979.

[15] Shutao Li, Bin Yang, Jianwen Hu, Performance comparison of Multi resolution transform for image fusion, Information Fusion 12, 2011, pp.74-84.

[16] Arthur L.da Cuncha,JIANPING Zhou, "The Nonsubsampled Contourlet transform: Theory, Design and Applications." IEEE Transcations on Image Processing, Vol 15, Oct2006.

[17] Ch.Hima Bindu, Dr.K.Satya Prasad, "MRI-PET medical image fusion by combining DWT and contourlet transform." To be published in Springer conference, Aug2012, ITC 2012, LNEE, pp. 124-129, 2012.

[18] Ch.Hima Bindu, et.al, "Discrete Wavelet Transform Based Medical Image Fusion using Spatial Frequency Techniques", International Conference on Recent Advances in Engineering and Technology (ICRAET 2012), Apr 2012.

[19] Ch.Hima Bindu, et.al, " Multimodal Medical Image Fusion of MRI-PET using wavelet transform." To be published in 2012 International Conference on Advances in Mobile Network, Communication and Its Applications Aug2012.

[20] Arthur L.da Cuncha,JIANPING Zhou, "The Non subsampled Contourlet transform: Theory, Design and Applications." IEEE Transactions on Image Processing, Vol 15, Oct2006.

[21] Candès, L. Demanet, D. Donoho, L.X. Ying, Fast discrete curvelet transforms, SIAM Multiscale Modeling and Simulation 5 (3) (2006) pp: 861–899.

[22] C.S. Xydeas, V. Petrovic, Objective image fusion performance measure, Electronic Letters 36 (4) (2000) 308–309.

AUTHORS PROFILE

Ch.Hima bindu is currently working as Associate Professor in ECE Department, QIS College of Engineering & Technology, ONGOLE, and Andhra Pradesh, India. She is working towards her Ph.D. at JNTUK, Kakinada, India. She received her M.Tech. from the same institute. She has ten years of experience of teaching undergraduate students and post graduate students. She has published 10 research papers in International journals and more than 8 research papers in National & International Conferences. Her research interests are in the areas of image Segmentation, image Feature Extraction and Signal Processing.

Dr.K.Satya Prasad is currently Rector and Professor in ECE Department, JNTUK, Kakinada, India. He received his Ph.D. from IIT, Madras. He has more than 32 years of experience in teaching and 25 years of R & D. He is an expert in Digital Signal Processing. He guided 10 PhD's and guiding 10 PhD scholars. He authored Electronic Devices and Circuits, Network Analysis and Signal & Systems text books. He held different positions in his carrier like Head of the Department, Vice Principal, Principal for JNTU Engg College and Director of Evaluation & presently the Rector of JNTUK.. He published more than 100 technical papers in national and International journals and conferences. The area of interest includes Digital Signal Processing, Image Processing, Communications etc.

Appendix A : Performance Analysis Tables

Table: I Evaluation of different methods for CT-MRI images

Algorithm	Mean	Std	Entropy (bits/sec)	Grad	Wrap	MI_{RI^F}	Corr	PSNR (db)	MI_F^{AB} (mean/std)	$Q^{AB/F}$ (mean/std)	Q_0 (mean/std)
Hybrid Approach	59.67	58.60	6.67	8.68	0	2.83	0.97	24.63	4.06	0.67	0.28
Non Subsampled Contourlet Transform	59.96	**60.51**	6.73	10.20	0.98	2.91	0.98	**25.95**	5.82	**0.77**	**0.31**
Fast Discrete Curvelet Transform	59.93	59.81	**6.79**	6.02	**0**	2.58	0.98	25.26	3.70	0.64	0.26
Contourlet	**60.13**	60.44	6.76	10.4	0	**2.94**	0.98	25.23	4.65	0.68	0.25
Discrete Wavele Transform	59.26	59.42	6.68	**10.56**	-1.38	2.46	0.94	21.19	3.43	0.47	0.27
PCA Method	52.16	53.53	6.55	7.75	-8.47	2.79	0.09	17.96	**5.86**	0.65	0.01
Pixel average	32.17	32.60	5.78	5.25	**-28.47**	2.86	**0.99**	15.55	5.05	0.38	0.02

Table: II Evaluation of different methods for MRI-PET images

Algorithm	Mean	Std	Entropy (bits/sec)	Grad	Wrap	MI_{RI}	Corr	PSNR (db)	MI_F^{AB} (mean/std)	$Q^{AB/F}$ (mean/std)	Q_0 (mean/std)
Hybrid Approach	27.70	56.78	3.09	5.64	-5.19	1.10	0.77	**63.15**	0.55	0.001	0.75
Non Subsampled Contourlet Transform	27.69	58.48	2.82	8.03	0.12	1.2	0.75	62.91	0.78	**0.054**	0.43
Fast Discrete Curvelet Transform	**27.90**	56.99	**3.46**	6.00	0.01	1.06	0.76	63.06	0.23	0.001	0.70
Contourlet	27.77	58.43	3.05	**8.06**	0.01	1.15	0.75	62.91	0.7	0.001	0.81
Discrete Wavele Transform	27.65	**58.49**	2.96	8.02	-5.4	10.22	0.75	62.91	1.38	0.001	0.98
PCA Method	27.54	58.27	2.77	8.01	0.18	6.06	0.73	56.72	**1.72**	0.003	0.99
Pixel average	13.92	29.36	2.77	4.01	**-0.05**	**11.06**	0.74	**63.15**	1.42	0.001	0.98
Brovary Method	8.42	25.47	2.15	2.22	0.13	0.74	**0.78**	58.13	1.35	0.001	**1**

Table: III Evaluation of different methods for CT-PET images

Algorithm	Mean	Std	Entropy (bits/sec)	Grad	Wrap	$MI_{RI}{}^{F}$	Corr	PSNR (db)	MI_{F}^{AB} (mean/std)	$Q^{AB/F}$ (mean/std)	Q_0 (mean/std)
Hybrid Approach	**45.65**	79.06	**4.94**	7.99	0.023	0.73	0.93	63.27	0.37	0.0004	0.9
Non Subsampled Contourlet Transform	45.6	80.91	4.73	10.95	0.56	0.77	0.95	65.26	0.59	0.0004	**1**
Fast Discrete Curvelet Transform	45.6	79.17	2.54	9.63	0.06	0.61	0.85	60.01	0.25	0.0005	0.005
Contourlet	45.53	81.05	1.99	11.3	0.029	0.74	0.93	63.51	0.42	0.0003	0.004
Discrete Wavelet Transform	**45.65**	**81.29**	1.25	**11.37**	0.001	**1.81**	**0.96**	**65.7**	0.97	0.0006	0.83
PCA Method	45.29	80.82	4.66	11.04	0.005	1.71	**0.96**	65.37	1.09	0.0006	0.004
Pixel average	42.37	52.09	4.36	4.46	0.007	1.34	**0.96**	65.4	1.09	0.0006	0.004
Brovary Method	20.09	57.68	2.45	5.83	**-0.371**	0.73	0.46	52.44	**1.51**	**0.0014**	0.92